Noise Mitigation Analysis of a Pi-Filter for an Automotive Control Module

Noise Mitigation Analysis of a π-filter for an Automotive Control Module

Cyrous Rostamzadeh [#1], Flavio Canavero [*2], Feraydune Kashefi [$3]

[#] *Robert Bosch LLC, Automotive Group,*
Farmington Hills, United States,
[1] Cyrous.Rostamzadeh@us.bosch.com

[*] *Politecnico di Torino,*
Torino, Italy
[2] flavio.canavero@polito.it

[$] *Khavaran Institute of Science & Technology,*
Mashhad, Iran
[3] Fred.Kashefi@gmail.com

***Abstract*—Electromagnetic interference (EMI) filters are often used on automotive 13.8 V_{DC} power networks to reduce high-frequency noise from being conducted off the printed circuit boards (PCB) and resulting into EMI problems. The filter performance is difficult to predict and often compromised at high frequencies due to parasitics associated with the filter itself, or the PCB layout. The power line filters with Surface Mount Technology ferrite and Multi Layer Ceramic Capacitors are attractive solutions for mitigation of RF noise in high-density automotive PCBs. A lumped-element SPICE model is introduced for optimized π-filter design, including frequency-dependent ferrite component model. The PCB implementation of EMI filter is outlined for optimum filter performance.**

I. Introduction

Switched mode power supplies (SMPS) are extensively used in automotive electronic modules due to their excellent efficiency, and have virtually eliminated the use of linear-regulator supplies. However, they are inherently noisy and generate ripple that require filters to meet stringent EMC specifications. Automotive EMC requirements [1, 2, 3, 4] are more stringent than FCC-15/J Class B limits by at least 54 dB [5]. The use of EMI filters as noise mitigation technique must be considered carefully; as cost and space in highly congested PCB's are two major determining factors. Discrete π-filters in small foot-print package are a common design practice by automotive design community. However, design and PCB implementation of EMI filter is not an easy task. Thus it is a major issue when a non-conformance is achieved with an EMI filter which fails to deliver the required noise mitigation[9,10].

π-filter that theoretically functions quite well using traditional circuit theory, or simulation tools, may fail to meet the rigor of its practical requirements (CE mitigation). It is often considered an art of black-magic when a well-designed EMI filter fails to function and deliver any noise reduction, as expected [11,12].

Therefore, it is necessary to consider and undertake an experimental approach to identify the *'technical errors'* which may cause the filter malfunction. Electrical behavior of an EMI filter mounted on a real product under the influence of complex input/output impedance variation, may differ substantially from its basic electrical schematic. In order to gain an insight into the realistic behavior of the EMI filter, one may consider the use of non-ideal electrical models for the filter components. However this can also be limited to provide a solution. Furthermore, considering the PCB parasitics due to the individual copper traces, or component interaction, can be difficult under a realistic product development budget, if not impossible. In every product development timeline, engineers are sought to find realistic, quick, and meaningful solutions. There are a large number of EMI filter design guidelines and best-practices available for engineering community. Product design team must deliver an EMI robust module, which must meet stringent EMI requirements that can be cost-effective, with little opportunity for any design iterations. In cost-effective, high-volume automotive world, it is absolutely essential to avoid the EMI failures and reduce design iterations. It is an extremely important aspect of automotive world as for engineer's ability to get it right in his first attempt. Nevertheless, an EMI filter design is considered here with components that do deviate from ideal behavior both in linear and non-linear fashion. The non-linear behavior is less understood or appreciated, more specifically, when ferrites are utilized on power distribution networks [13,14]. Suppliers of SMT ferrites provide impedance characteristics *vs* frequency, and in addition, several lumped circuit models are offered to help the design engineers for the SPICE simulation purpose [6,15].

In ideal world, a π-filter provides a perfect solution to EMI generated noise, more specifically, for noise reduction due to conducted RF emission resulting from switched mode power supplies. The major concern is the MW-AM band radio (0.52 MHz – 1.73 MHz). Currently SMPS operate anywhere from

978-1-4244-6307-7/10/$26.00 ©2010 IEEE

100's of kHz to 2 MHz of switching frequencies. The main concern is the first few harmonics of the SMPS switching frequencies in which it may cause EMI non-conformance.

II. Product EMI Compliance Measurements

This Section presents an examination of the fundamental problems encountered during the EMI compliance assessment of an automotive safety restraint control, that failed to meet the conducted emission requirements.

A typical airbag restraint module was designed on a printed circuit board consisting of four layers of copper, fabricated on FR4 substrate, to accommodate for the component population in excess of 500. One layer of PCB is dedicated to a return (ground) plane. A host of low speed signal traces, power distribution nets, high-speed communication nets, PWM-based sensor communication, and in addition, HS-CAN Bus communication were connected in the remaining inner and outer layers. Unused gaps were filled with copper traces or copper islands. The 'ground-filled' gaps were "stitched" to the return plane using a large number of vias distributed frequently at less than 1-cm apart.

Fig. 1 illustrates the noise spectral content where a deviation was recorded at the harmonics of 390 kHz (SMPS switching frequency).

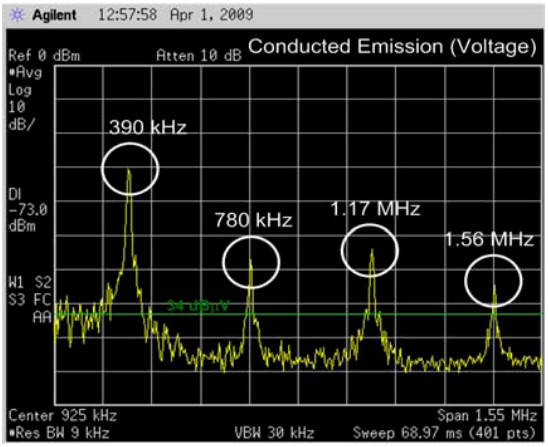

Fig. 1. Conducted Emission (Voltage) Pre-Compliance Average Detector, Limit @ 34 dBμV

A diagnostic effort to identify, determine and isolate the noise source, and its conducted path, was easily reduced to the input port of a boost converter operating at 390 kHz. It was recognized that a simple third order EMI filter with 60 dB of insertion loss (MW-AM band) may be required for the unit under test to meet the CE requirements. In its simplest form, an EMI filter is an impedance discontinuity network inserted at the input port of 13.8 V DC battery or ignition line. As a result of EMI filter, it provides required attenuation to noise signals that may cause non-conformance during a Conducted Emission test.

A π-filter topology is a common design practice in most automotive noise mitigation design techniques. The π-filter network was designed using 0603 SMT ferrite bead and two identical 4.7 μF, 1210 multi layer ceramic capacitor (MLCC) to provide the insertion loss required in the frequency band of interest. However, it appears that EMI-filter behaves rather unpredictably, and this is not an acceptable situation. Design Engineers with little EMC training, would resort to statements that are difficult to grasp, and for most engineers it is discouraging to engage in a ghost-finding scenario.

In order to eliminate, or reduce, the inconvenience of EMI qualification of a poor filter design for noise mitigation, a systematic approach was outlined to assess the success of a design. As number of iterations attempted by replacing the filter components can be problematic and costly, it is insightful to seek for a technical guidance which produces a high-rate of success. The questions that need to be answered:

1. Why lumped model simulation fails to address the test outcome?
2. Why incorporation of non-ideal behavior of filter components cannot solve/answer the filter misbehavior?
3. Is there a conflict in 'PCB design guideline' that results in poor filter performance?

III. π– Filter Characteristics

SMT Ferrite Beads as frequency-selective nonlinear devices have the potential to solve a large range of interference problems. Unlike a magnetic metal, a ferrite is a magnetic dielectric that allows an electromagnetic wave to penetrate the ferrite, thereby permitting an interaction between the wave and magnetization within the ferrite. Ferrites are non-conductive ceramic materials made by sintering a mixture of iron oxides with either oxides of zinc or nickel and zinc. Fig. 2 illustrates the impedance characteristics of 0603 SMT ferrite bead selected for π-filter application.

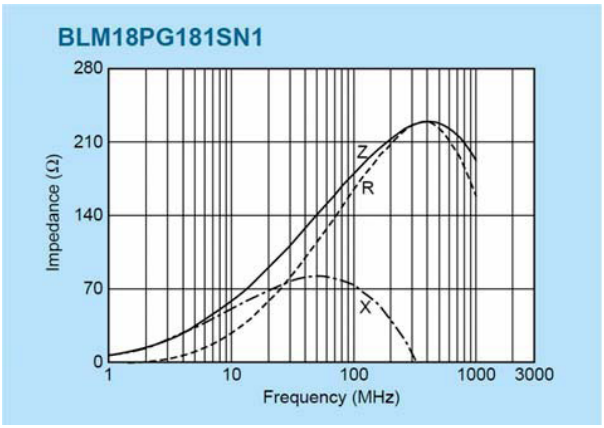

Fig. 2. SMT 0603 Chip Ferrite Bead Impedance - Frequency Characteristics

Impedance of the SMT ferrite bead for this application is 181 Ω @ 100 MHz, as in Fig. 2. It is evident that at lower frequencies (less than 25 MHz) inductance of the bead is the dominant term. In the frequency range between 25 MHz and 400 MHz, the frequency-dependent, resistive, dissipative element dominates the impedance characteristics. At higher

frequencies (above 400 MHz), parasitic capacitance of the SMT ferrite structure is the dominant term.

Fig. 3 is an illustration of a simple electrical equivalent circuit lumped-model supplied by ferrite bead manufacturers. It is assumed that the values provided for the equivalent circuit model is only valid at the frequency of 100 MHz. Indeed, the model is a very simple representation of the actual electrical behavior, and does not represent the frequency dependent terms and should be used with this limitation. Nevertheless, it is a common practice to examine the ferrites @ 100 MHz.

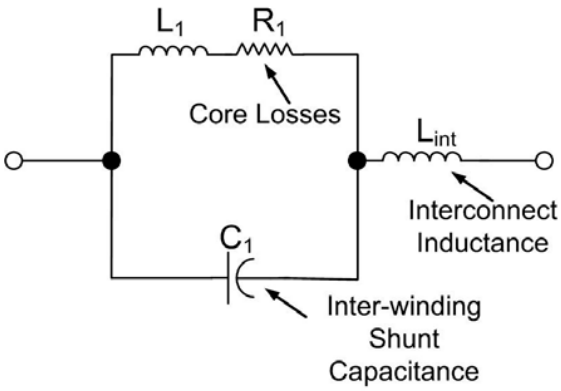

Fig. 3. BLM18PG181SN1 Electrical Lumped Circuit Model

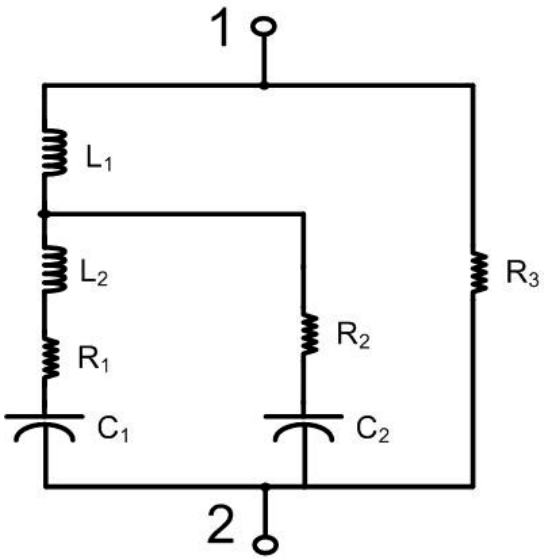

Fig. 4. MLCC (4.7 µF) Equivalent Circuit Model

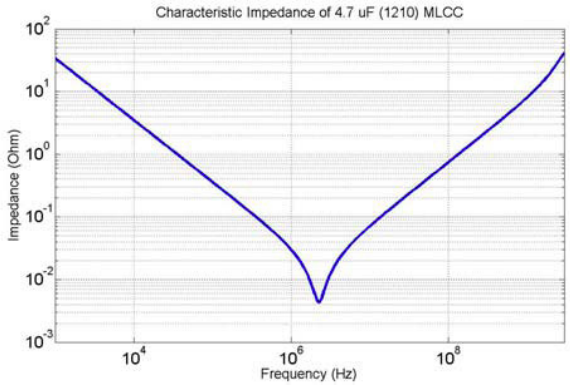

Fig. 5. MLCC 1210, 4.7 µF Impedance Characteristic

Two 4.7 µF@25V SMT X7R (1210, 3.2 mm × 2.5 mm) MLC parallel capacitors [7] complete the structure of the π-filter. Fig. 4 is an illustration of the equivalent circuit model for the adopted capacitor and Table 1 provides the individual component values at 2.29 MHz (SRF frequency). Fig. 5 illustrates the impedance-frequency characteristic of 4.7 µF MLC capacitor.

TABLE 1.

MLCC 1210 (4.7 µF) MODEL COMPONENT VALUES

L1	56 pH
L2	1.06 nH
C1	4.23 µF
C2	6.5 pF
R1	4.28 mΩ
R2	49.69 Ω
R3	212.76 x 10^6 Ω

Utilizing the electrical model and component values provided as in preceding figures, one can develop a simple π-filter circuit simulation using PSPICE to assess the effectiveness of the EMI filter in the conducted emission frequency range. Indeed, one such simulation demonstrates an incredible 80 dB of insertion loss throughout the AM frequency band. The realistic objective would require us to demonstrate a practical application where an 80 dB of insertion loss can be realized. If not, what are the limitations? In order to investigate this further, a 2-sided test PCB (67 mm X 52 mm) was constructed as illustrated in Fig. 6. The lower side of the PCB was dedicated to a solid copper (return plane). A 2.8 mm wide 30 mm long PCB trace was realized and terminated into SMA ports with filter components attached as illustrated in Fig. 6.

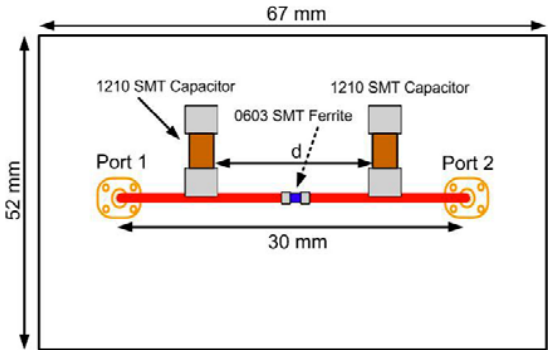

Fig. 6. π-Filter Test Circuit Printed Circuit Board Geometry

A calibrated network analyser (HP8753D) was utilized to measure the voltage transfer function ($|S_{21}|$) of the π-filter structure as in the test PCB.

The SMT ferrite bead was removed and replaced with a 2.7 nH ceramic core inductor and voltage transfer function ($|S_{21}|$) was captured. In addition, a large 4.7 μH ferrite core inductor was substituted for the 0603 ferrite bead and voltage transfer function ($|S_{21}|$) was recorded. Fig. 7 illustrates the post-processed data.

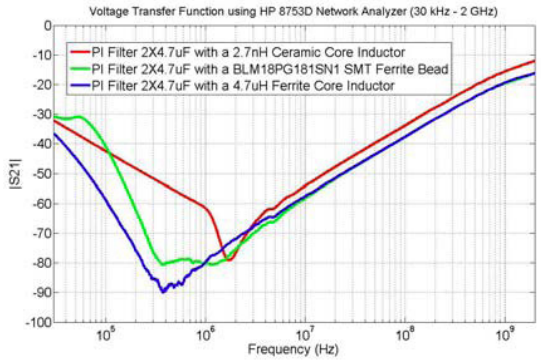

Fig. 7. Voltage Transfer Function of π-Filters

In addition, quality factor of 2.7 nH ceramic core inductor and ferrite bead was measured at 800 MHz: the 2.7 nH Ceramic Core 0805 Inductor gave Q ~ 63, considered "High-Q", and the BLM18PG181SN1 Ferrite SMT 0603 resulted in Q ~ 0.68, considered "Low-Q". It is a fundamental EMI filter design guideline to avoid the use of high-Q components. Therefore, the use of ceramic core inductor must be avoided.

It is clear that large and expensive 4.7 μH inductor at lower frequencies (below 1 MHz) has a superior performance, compared with the ferrite bead, as expected. However, it is important to note that for frequencies greater than 1 MHz, ferrite bead is as effective as large inductor, and in the frequency range (1 MHz – 10 MHz) it outperforms the large inductor by 3 dB. It is evident that small 2.7 nH ceramic core inductor is not effective at MW-AM band and should be avoided. The measured data in the "experimental PCB" is useful for design engineers to assess the filter effectiveness and provide design guidelines.

IV. Automotive PCB

The product PCB implementation of π-filter is illustrated in this Section. Implementation rules prescribe that automotive electronic products are required to operate reliably under harsh environmental conditions. In several applications, printed circuit boards are treated via conformal coating to protect PCB and its electronic components. Several important manufacturing requirements would result due to conformal coating process. For example, one important rule would require the PCB design engineer to avoid placement of via(s) under the electrolytic capacitors. Electrolytic capacitors have failure modes associated with chemical leakage. An incorrect electrolyte formula within a faulty capacitor causes the production of hydrogen gas, leading to bulging or deformation of the capacitor's case, and eventual venting of the electrolyte. In the event of capacitor failure, a catastrophic electrical short circuit would result from the ground-fill island and through vias to PCB ground plane. In the electronic restraint control module, a large size electrolytic capacitor (6.7 mF/25V_{DC}) is required for airbag deployment during loss of input power. Airbag deployment function cannot be compromised if vehicle power delivery system was interrupted. In a high density printed circuit board, 6.7 mF/25V_{DC} electrolytic energy reserve capacitor is indeed the largest physical component.

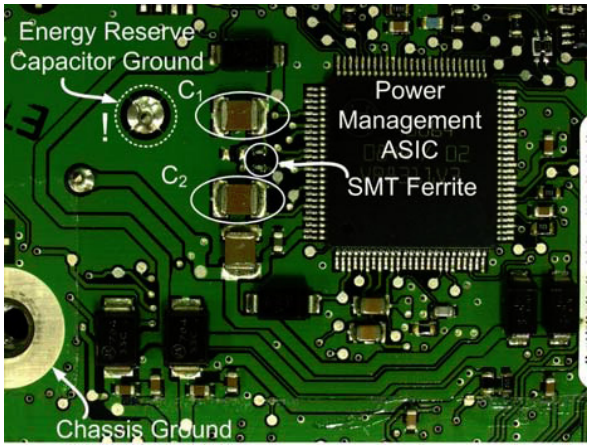

Fig. 8. Printed Circuit Board (Board #1)

The integration of the π-filter is illustrated in Fig. 8, where the location of C_1, C_2 and SMT ferrite components is indicated. π-filter components are arranged in the close proximity of the power management ASIC and chassis ground. The energy reserve capacitor (6.7 mF aluminium electrolytic) was mounted on the opposite side of the PCB. The energy reserve capacitor ground is illustrated in the PCB picture. It is important to note the absence of vias in the "copper island" pertaining to energy reserve capacitor ground, and EMI filter C_1, C_2 ground connections. Fundamental EMC design guidelines require the ground-filled copper islands to be stitched to the ground plane using multiple vias. However, this requirement cannot be implemented here, as it is mandatory to avoid placement of vias for the manufacturing requirements of

all the conformal coated printed circuit boards, as outlined earlier in this paragraph.

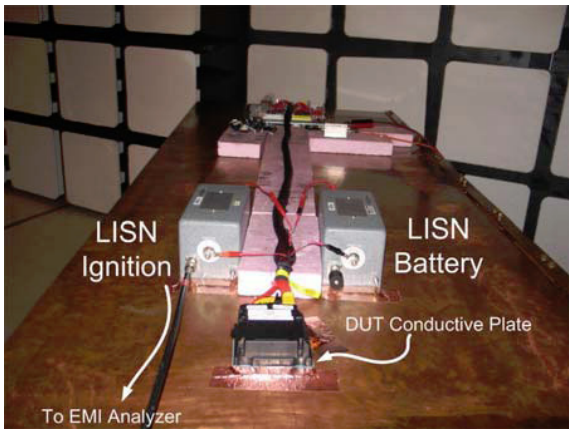

Fig. 9. CISPR 25 Conducted Emission (Voltage) Test Setup

For EMI compliance, the product needs to be tested according to regulations. Conducted RF Emission test setup complies with the requirements of CISPR 25 [8] and is illustrated as in Fig. 9. It is important to note that safety restraint control module is electrically bonded to the vehicle body during the production through the base plate case. Therefore the DUT is placed directly on the CISPR 25 ground plane and bonded with the ground plane as seen on the setup picture. Test harness is 1700 (+300, -0) mm long and routed 50 mm above the ground plane.

Automotive Line Impedance Stabilization Network (LISN) for electrical schematic is shown in Fig. 10.

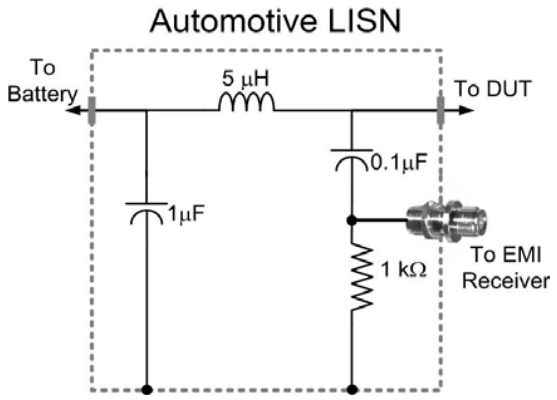

Fig. 10. Automotive 50 Ω LISN Schematic

Conducted noise measurements for the PCB #1 was presented earlier in Fig. 1. It is clear that the PCB board #1 implementation exceeds the CE compliance requirements at SMPS switching frequency and its harmonics. A number of changes to the EMI component values, or types, failed to mitigate the CE noise. It is a fundamental EMI design guideline to position the π-filter components at the power entry pin, and electrically bond to the chassis ground with a low impedance connection. It is clear that the filter components are strategically located as required per EMI guidelines. In order to investigate the effectiveness of the EMI filter, it was decided to remove the filter components, and replace the ferrite bead with a 20 mΩ resistor. The CE noise spectral content, and its amplitude, remained identical in both scenarios. Indeed, the presence or absence of the EMI filter resulted in identical CE data, revealing a serious design error. It was suggested that the implementation of the EMI filter on PCB board #1 was radically different from the test board (Fig. 6), or simulation results. Therefore, EMI filter electrical behaviour was difficult to predict and it cannot be explained using conventional electrical network theory.

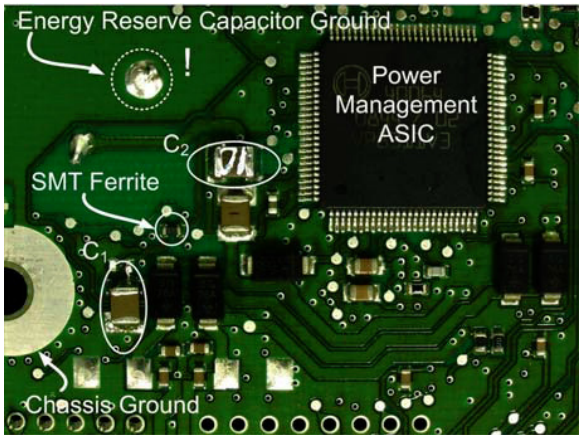

Fig. 11. Printed Circuit Board (Board #2)

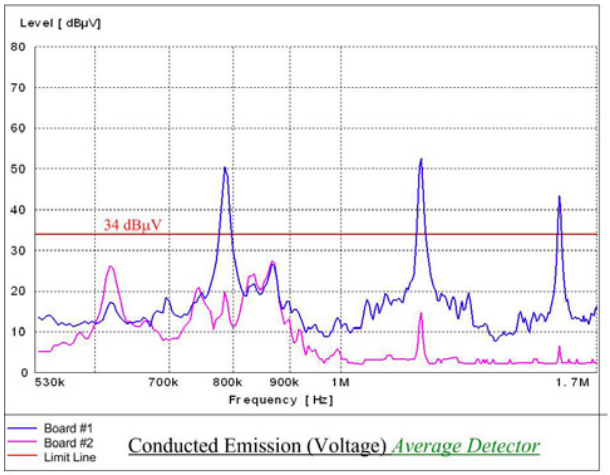

Fig. 12. Comparison of Conducted Emissions (Voltage) of Board #1 and #2; Measurements in the MW-AM Band

In one final attempt, EMI filter components were removed and placed on a small (1 cm × 1 cm) 2-sided PCB, with lower side dedicated to return plane. The modified small EMI-filter PCB was placed over the main product PCB board, and configured between the ASIC power input pin, and the module power input pin. EMI-filter PCB was connected to main PCB ground structure at "chassis ground" with a short wire to reduce connection inductance. The CE measurements

with this modification resulted in a 40 dB of suppression of SMPS noise components. Therefore, the EMI filter implementation of PCB board #1 required major analysis.

Printed circuit board #2 illustrated in Fig. 11, was developed as a result of the CE failures observed in the previous PCB and Fig. 12 illustrates the CE measurements for both printed circuit boards. It is clear that PCB #2 meets the EMI requirements and provides the performance as expected from electrical simulations and measurements in the test PCB.

V. Analysis

A close examination of Fig. 8 and Fig. 11 reveals the most critical differences between two different printed circuit boards. It is important to note that the ground connection of π-filter capacitor C_1 plays an important role in the effectiveness of the EMI filter. In Fig. 8, referring to PCB board #1, C_1 and large energy reserve capacitor are connected to the same "ground copper island". The presence of the high-frequency charge currents (490 kHz and its harmonics) for the energy reserve capacitor is a major problem for the "ground copper island". Further investigation of the C_1 using an Agilent 85024A high-frequency current probe, revealed the presence of SMPS noise currents. It is required to find a reference plane which is relatively free from high-frequency RF currents, and EMI filter must be referenced to the RF-free reference plane, i.e, chassis or 'quiet ground'. It is obvious that the "ground copper island" cannot be termed as ideal, or chassis ground. In order to verify the filter ground concept, several short electrical connections were introduced between the "ground copper island" and chassis ground and measured CE data revealed an astounding improvement in the behavior of the filter. As a result of the reported investigation, PCB #2 was designed and CE data is presented in Fig. 12. It is evident that the PCB #2 provides 40 dB of noise mitigation as required. It is important to note the mounting strategy and ground connection of EMI filter capacitors are critical.

VI. Conclusion

This study is an examination of the fundamental problems encountered in simple EMI filter implementations for printed circuit boards. Engineers are confronted to design products for automotive applications under harsh environmental conditions with stringent EMI requirements. Analytical tools can be limited to provide required guidelines for engineers to develop automotive products with multiple requirements, often in conflict with one another. In this report, an error in the PCB implementation of π-filter is outlined due to manufacturing requirements which overrides best EMI practices. The engineer's ability to adhere to low-cost technology with solutions to thermal, EMI, manufacturing constraints and several other major requirements determines the success of an automotive product.

References

[1] Ford Motor Company (EMC-CS-2009, September 2009).

[2] General Motors Corporation (GMW3097 Rev. 5, May 2006).

[3] DaimlerChrysler Corporation (DC-11224, May 2007).

[4] Chrysler Corporation (CS-11809, May 2009).

[5] C. Rostamzadeh, S. Connor, B. Archambeault, "Numerical and Experimental Investigation of Power Supply Noise Decoupling Strategies on Single-Sided Printed Circuit Boards," in *Proc. EMC 2007 IEEE International Symposium*, Honolulu, Hawaii, Jul 9-13, 2007, pp. 1-5..

[6] K. Keskinen, "Modeling a Ferrite Bead on High Speed Serial Links," CORESIM Inc., April 14, 2004

[7] C. Rostamzadeh, H. Dadgostar, F. Canavero, "Electrostatic Discharge Analysis of Multi Layer Ceramic Capacitors," in *Proc. EMC 2009 IEEE International Symposium*, Austin, TX, Aug 17-21, 2009, pp. 35-40.

[8] CISPR 25 Edition 3.0, March 2008, IEC Central Office, Geneva, Switzerland.

[9] Keenan, A., "Board level EMI suppression using ferrite components," *Electromagnetic Compatibility, 2003. EMC '03. 2003 IEEE International Symposium on* , vol.2, no., pp. 1252-1254 Vol.2, 11-16 May 2003.

[10] Arafiles, V.P., "Reducing high frequency conducted noise," *Electromagnetic Compatibility, 2002. EMC 2002. IEEE International Symposium on* , vol.1, no., pp.334-339 vol.1, 19-23 Aug. 2002.

[11] Hill, L.; Bruce, J., "Utilizing overlooked characteristics of ferrites for improved printed circuit board EMI suppression," *Electromagnetic Compatibility, 2006. EMC-Zurich 2006. 17th International Zurich Symposium on,* pp.383-386, Feb. 27 2006-March 3 2006.

[12] Jun Fan; Shaofeng, L.; Drewniak, J.L., "Including SMT ferrite beads in DC power bus and high-speed I/O line modeling," *Electromagnetic Compatibility, 2001. EMC. 2001 IEEE International Symposium on*, vol.1, no., pp.336-339 vol.1, 2001.

[13] Roc'h, A.; Iannarelli, R.; Leferink, F., "New materials for inductors," *Electromagnetic Compatibility - EMC Europe, 2009 International Symposium on*, vol., no., pp.1-4, 11-12 June 2009.

[14] Ho, B.; See, K.Y.; Chang, W.Y., "Measurement of EMI suppression of a ferrite core under realistic operating conditions," *Electromagnetic Compatibility Newsletter,* no.218, pp.60-65, Summer 2008.

[15] Qin Yu; Holmes, T.W.; Naishadham, K., "RF equivalent circuit modeling of ferrite-core inductors and characterization of core materials," *Electromagnetic Compatibility, IEEE Transactions on*, vol.44, no.1, pp.258-262, Feb 2002.